Supporting Information

Crystal Facet Effects of Platinum Single-Atom Catalyst in Hydrolytic Dehydrogenation of Ammonia Borane

Qingdi Sun,[a] Xuyu Wang,[b] Hao Wang,[a] Hao Zhang,[a] Qian He,[a] Ying Zhang,[a] Yujie Cheng,[a] Xingcong Zhang,[a] Shaolin Shi,[c] Leiming Tao,[e] Xiaohui He[a, d*] and Hongbing Jia[c, d*]

[a] *Fine Chemical Industry Research Institute, School of Chemistry, Sun Yat-Sen University, Guangzhou 510275, Guangdong, China.*

[b] *School of Environmental and Chemical Engineering, Jiangsu University of Science and Technology, Zhenjiang, 212003, China*

[c] *School of Chemistry and Chemical Engineering, Guangxi University, Nanning 530004, China*

[d] *Huizhou Research Institute of Sun Yat-sen University, Huizhou 516216, China.*

[e] *School of Chemical Engineering, Guangdong University of Petrochemical Technology, Maoming 525000, China.*

E-mail: jihb@mail.sysu.edu.cn; hexiaohui@mail.sysu.cn

Experimental Section

1. Catalysts Preparation.

1.1. Synthesis of Co_3O_4-x (x = c, t, o; Co_3O_4 cubic (Co_3O_4-c), Co_3O_4 truncated octahedron (Co_3O_4-t), and Co_3O_4 octahedron (Co_3O_4-o)).

For the synthesis of Co_3O_4-c, 0.4 g of NaOH and 11.72 g $Co(NO_3)_2$ were dissolved in 40 mL distilled water. The suspension was transferred into a 100 mL Teflon-lined stainless-steel autoclave then heated at 180 ℃ for 5 h.[1] The amount of 1.69 g $H_2C_2O_4$, 2.0 g NaOH and 24.72 g $Co(NO_3)_2$ mixed in 70 mL distilled water was for the preparation of Co_3O_4-t.[2] For the preparation of Co_3O_4-o, 2.0 g $Na_2C_2O_4$, 0.8 g NaOH and 24.72 g $Co(NO_3)_2$ were added in 70 mL distilled water. Then the two mixtures mentioned before were transferred into an autoclave and heated at 220 °C for 20 h. After the autoclaves were cooled to room temperature, the two precipitates were collected and washed several times with distilled water and ethanol, separately. Subsequently, all the products were dried at 60 °C for 5 h and then calcined in air at 500 °C for 3 h.[2]

1.2. Synthesis of Pt_1/Co_3O_4-x (x = c, t, o).

An impregnation method was applied to load Pt on Co_3O_4 substrates. A certain amount of Co_3O_4 was dispersed in a solution containing $[Pt(NH_3)_4](NO_3)_2$ (Pt loadings of 0.2 wt%). The pH of this suspension was adjusted to 8 by adding diluted ammonium solution. Thereafter, the mixture was stirred continuously into a constant temperature water bath at 50 °C for 3 h. By centrifugal filtering and washing, the products were collected and dried at 60 °C for 5 h. Finally, the catalyst was calcined in air at 400 °C for 2 h.[3]

2. Catalysts Characterization.

The XRD patterns were recorded by RIGAKU D-MAX 2200 VPC X-ray diffractometer with Cu-K_α radiation at 40 kV and 40 mA in the 2θ range of 10 to 80 ° with scanning rates of 10 °/min. The specific surface area of all the catalysts was measured by 3H-2000PM2 (Beijing Beishide) using the Brunauer-Emmett-Teller (BET) method. from the N_2 adsorption/desorption isotherms at -196 °C. The pretreatment of these samples was degassed at 180 °C for 4 h. The Pt loading was analyzed by ICP-OES instrument (AGILENT, ICP-OES730). Zeiss Field-Emission-SEM Gemini 500 and Quanta 400F were applied to confirm the morphology of the catalysts. Transmission electron microscopy (TEM) measurement was carried out on a JEM-2100F (JEOL, Japan) apparatus. JEOL ARM200F equipped with an EDX detector (JEOL) and an energy filter (GATAN) was used for HAADF-STEM imaging and elemental mapping of the samples. AC HAADF-STEM images were conducted on a JEM-ARM200F TEM/STEM with a guaranteed resolution of 0.08 nm. X-ray photoelectron spectroscopy (XPS) data were conducted on the Thermo Scientific™

Nexsa™ (USA) spectrometer with a monochromatized Al Kα source, and the C 1s peak at 284.6 eV was applied to make an energy calibration. Diffuse reflectance infrared Fourier transform spectroscopy (DRIFTS) of CO chemisorption measurements were performed on a Bruker VERTEX 70v spectrometer. The sample was first pretreated in 10% O_2 in Ar at 150 °C to remove any contaminant. After cooling the sample to room temperature under Ar, a background spectrum was collected. Then the sample was exposed to 10% CO in Ar at a flow rate of 20 mL/min for about 30 min until saturation. Next, Ar (99.999%) was introduced at a flow rate of 20 mL/min for another 30 min to remove the gas-phase CO, and then the DRIFT spectrum was collected with 256 scans at a resolution of 4 cm^{-1}. The *in-situ* DRIFTS spectra were collected on Nicolet iS20 spectrometer. 10 mg catalysts were tableted and transferred to the *in-situ* infrared tube. AB solution was dropped on the catalysts sheet for detection. Hydrogen temperature-programmed reduction (H_2-TPR) was performed on a Micromeritics Autochem II 2920 instrument. Each sample was first pretreated in 10% O_2 in Ar at 200 °C for 60 min. Next, the sample was cooled to 0 °C in Ar and wait for 30 min until the baseline became stable. TPR was performed by heating the sample at 10 °C/min up to 550 °C in 10% H_2 in Ar and a cooled trap with an isopropyl alcohol/liquid nitrogen slurry at -80 ˚C was used before the TCD detector to retain the produced water.

3. Catalyst Activity Measurement.

The hydrogen evolution of ammonia borane was conducted in a homemade gas generation setup. The hydrolytic dehydrogenation of ammonia borane (AB, Bidepharm 97%) was kept in a schlenk reactor at room temperature (~ 30 °C) under atmospheric pressure. Typically, 20 mg of the Pt_1/Co_3O_4-c and Pt_1/Co_3O_4-c, Pt_1/Co_3O_4-o catalyst with the same amount of metal content was added in the reactor. Then, 2 mL aqueous AB solution (16.3×10^{-2} M) was introduced into the reactor through a constant pressure funnel. A magnetic stirrer was employed to mix the AB solution and the catalyst. A water-filled burette was used to measure the generated volume of H_2. The turnover frequency (TOF) was calculated with the time while generating 17 mL of H_2 according to the equation:

$$TOF = \frac{n_{gas}}{n_{metal}} \cdot \frac{1}{t} \qquad \text{Eq (1)}$$

Here n_{gas} is the mole of generated H_2, while n_{metal} is the total mole of Pt in the sample. t is the reaction time in min. According to the repeatability test, after the hydrogen generation reaction was finished, another equivalent amount of AB was added into the schlenk reactor. Then the generated volume of H_2 by the water-filled gas burette with reaction time was recorded. Similar operations were repeated 10 times. For kinetic studies, the hydrolytic dehydrogenation of AB reaction was also carried out at 35, 40, and 45 °C, to obtain the activation energy (E_a).

4. Computational Details.

All the calculations were performed by spin-polarized density functional theory (DFT) as implemented in the Vienna ab initio simulation package (VASP).[4-7] The exchange-correlation interaction is described by the generalized gradient approximation (GGA) with the Perdew–Burke–Ernzerhof (PBE) functional.[8] A kinetic cutoff energy of 450 eV with (3 × 2 × 1) Gamma *k* points was applied for plane wave expansions. The convergence criteria for the total energy and the forces were set as 10^{-5} eV and 0.02 eV $Å^{-1}$, respectively. DFT + U corrections with U_{eff} = 3.5eV were applied for Co 3d-orbitals, which was applied by Lu and co-wokrers[9] for the aim of providing a better overall description of electronic properties and surface reactivity. After optimizing, the bulk structure with a lattice parameter of 8.1134 Å was used to build the surface models. Co_3O_4 (100) and (111) surface was constructed as a p ($\sqrt{2} \times \sqrt{2}$) surface supercell with a 9 atom layers structure and a vacuum layer of 20 Å.[10, 11] During the whole calculation the bottom 3 layers were fixed, other atoms were fully relaxed. The metric for calculating the adsorption energy was as shown: $E_{ads} = E_{(adsorbate/catalysts)} - E_{adsorbrate} - E_{catalysts}$. Here the $E_{adsorbate/catalysts}$ was the total energy of AB/H_2 adsorption models, the $E_{adsorbrate}$ represented the energy of AB/H_2 molecular, and the $E_{catalysts}$ was the energy of the surface model of catalysts. Atomic charges were computed using the atom-in-molecule (AIM) scheme proposed by Bader.[12]

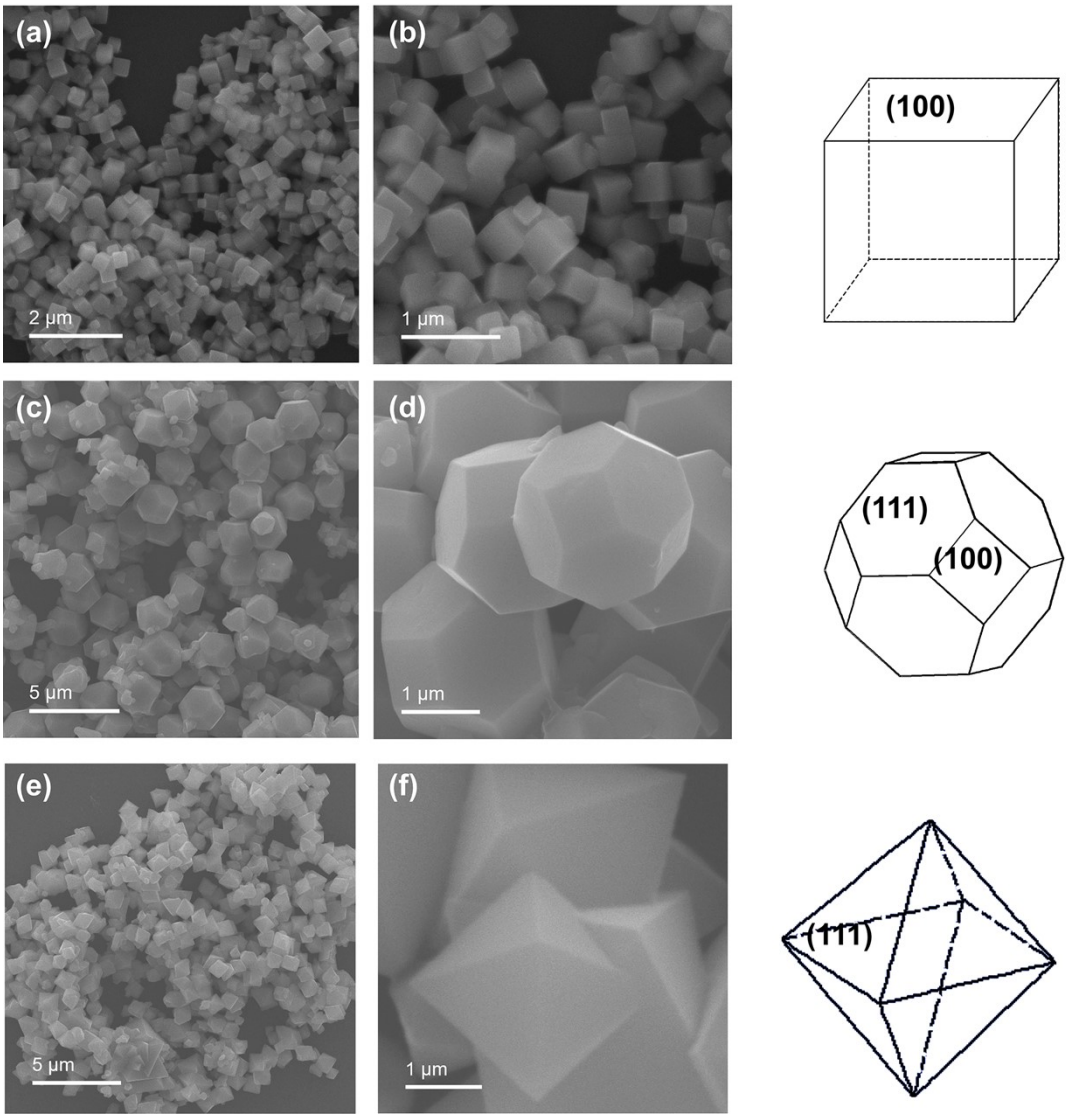

Figure S1. (a, b) SEM images Co_3O_4-c. (c, d) SEM images of Co_3O_4-t. (e, f) SEM images of Co_3O_4-o.

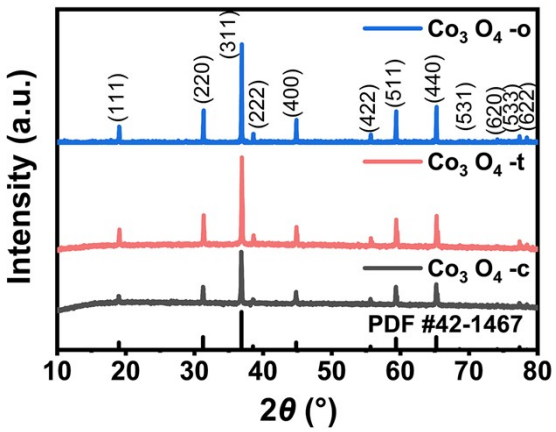

Figure S2. XRD patterns of Co_3O_4-c, Co_3O_4-t, and Co_3O_4-o.

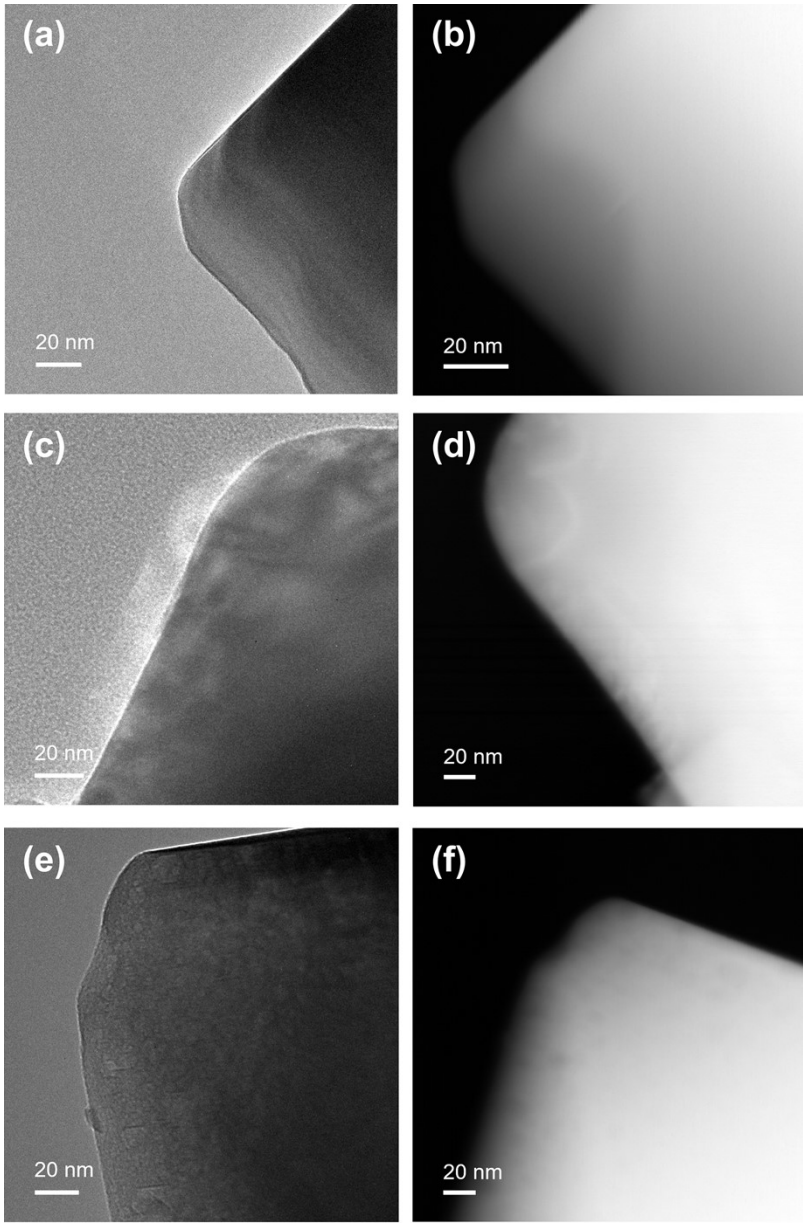

Figure S3. (a, c, e) TEM images of Pt_1/Co_3O_4-x (x = c, t, o), respectively. (b, d, f,) STEM images of Pt_1/Co_3O_4-x (x = c, t, o), respectively.

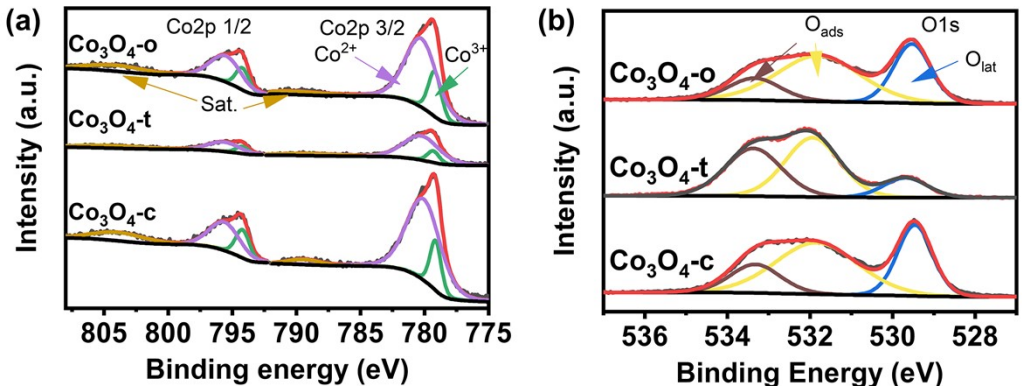

Figure S4. XPS spectra of Co_3O_4-x (x = c, t, o): (a) are Co 2*p* spectrums; (b) are O 1*s* spectrums.

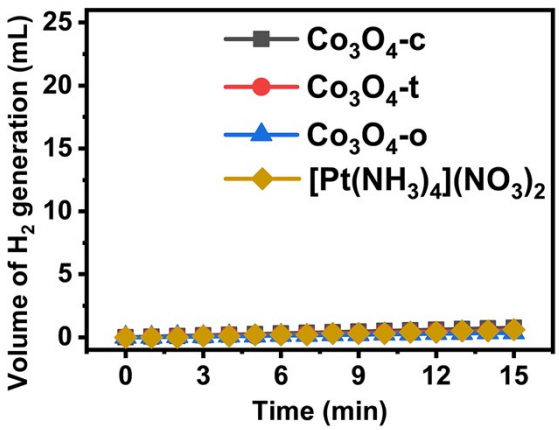

Figure S5. Curves of hydrogen generation versus time in the presence of Co_3O_4-x (x = c, t, o) and $[Pt(NH_3)_4](NO_3)_2$ at room temperature.

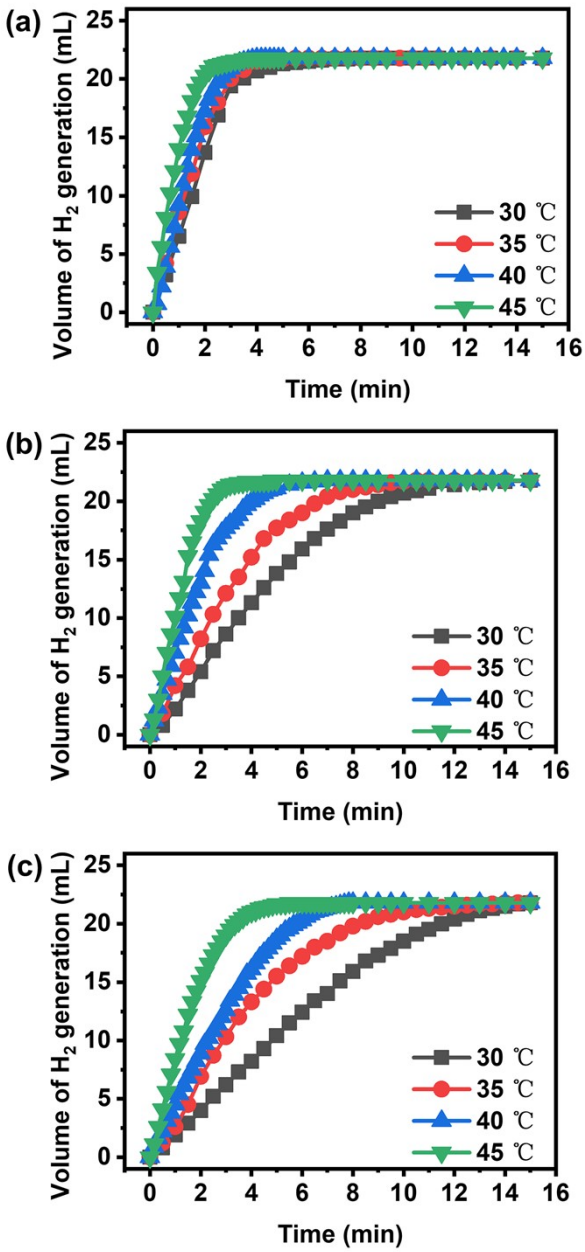

Figure S6. (a) Curves of hydrogen generation versus time in the presence of Pt_1/Co_3O_4-c at 30 °C,35 °C,40 °C,45 °C. (b) Curves of hydrogen generation versus time in the presence of Pt_1/Co_3O_4-t at 30 °C,35 °C,40 °C,45 °C. Curves of hydrogen generation versus time in the presence of Pt_1/Co_3O_4-o at 30 °C,35 °C,40 °C,45 °C.

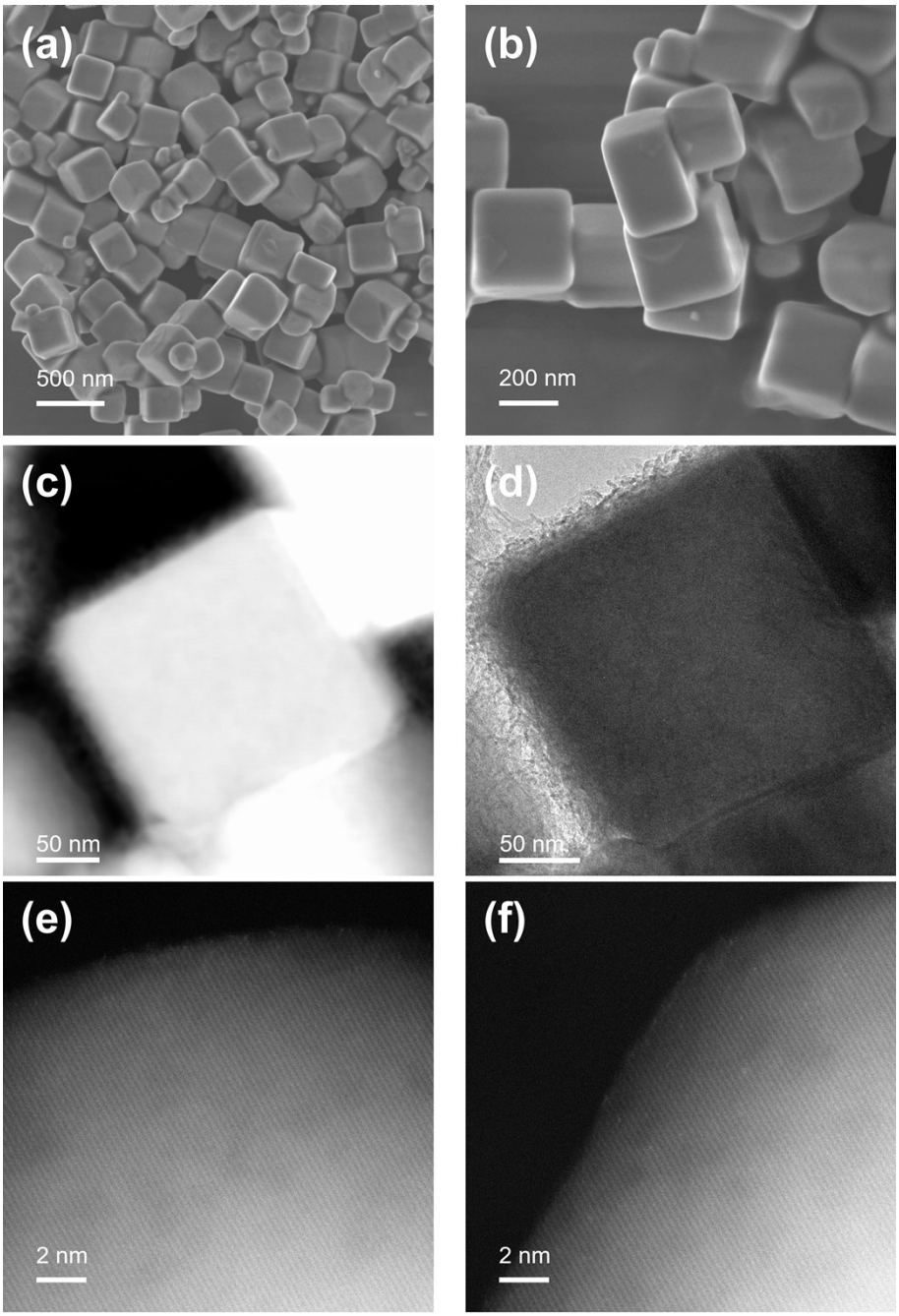

Figure S7. (a)(b) SEM images of the spent Pt_1/Co_3O_4-c catalysts. (c)(d) STEM and TEM image of the spent Pt_1/Co_3O_4-c catalysts. (e)(f) AC HAADF STEM images of the spent Pt_1/Co_3O_4-c catalysts.

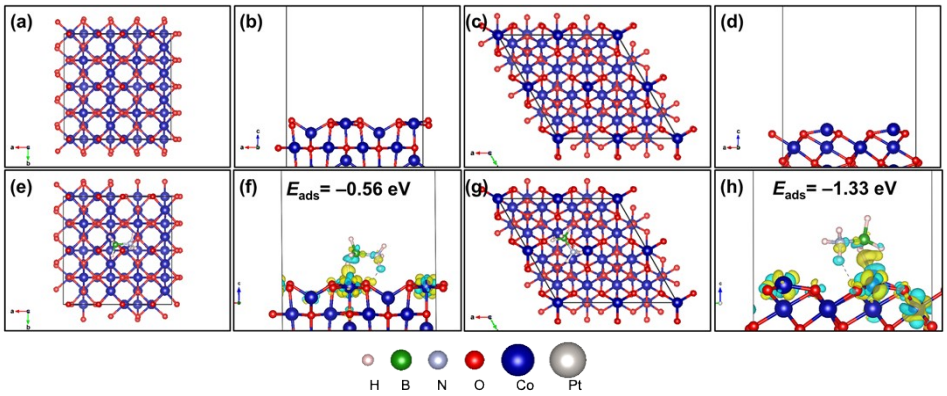

Figure S8. (a, c) are the top view of the Co_3O_4-(100) and Co_3O_4-(111) model. (b, d) are the side views of the Co_3O_4-(100) and Co_3O_4-(111) model. (e, g) are the top view of the AB adsorption model on the Co_3O_4-(100) and Co_3O_4-(111) surface, respectively. (f, h) are the charge density difference of AB adsorption models on the Co_3O_4-(100) and Co_3O_4-(111) surface, respectively. The yellow and blue regions refer to increased and decreased charge distributions, respectively.

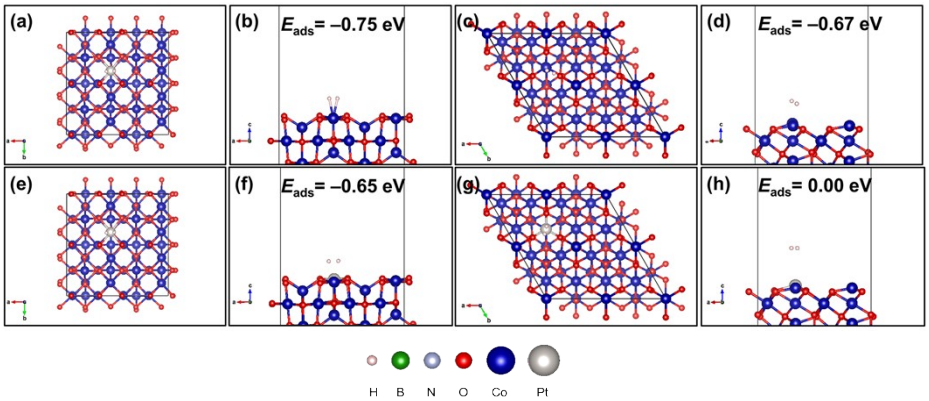

Figure S9. (a, c) are the top view of the H_2 adsorption models on the Co_3O_4-(100) and Co_3O_4-(111) surface, respectively. (b, d) are the side view of the H_2 adsorption models on the Co_3O_4-(100) and Co_3O_4-(111) surface, respectively. (e, g) are the top view of the H_2 adsorption models on the Pt_1/Co_3O_4-(100) and Pt_1/Co_3O_4-(111) surface, respectively. (f, h) are the side view of the H_2 adsorption models on the Pt_1/Co_3O_4-(100) and Pt_1/Co_3O_4-(111) surface, respectively.

Table S1. Pt loadings, S_{BET}, and the surface Pt species ratio of various catalysts

Catalysts	Pt	S_{BET}	Surface Pt species ratio
	wt%	($m^2\ g^{-1}$)	(Pt^{4+}/Pt^{2+})
Co_3O_4-c	- -	12.7	- -
Co_3O_4-t	- -	14.0	- -
Co_3O_4-o	- -	16.1	- -
Pt_1/Co_3O_4-c	0.05	14.9	5.6
Pt_1/Co_3O_4-t	0.13	13.4	2.9
Pt_1/Co_3O_4-o	0.15	14.3	2.6

Table S2. The turnover frequency (TOF) in units of mol_{H2} mol_{Pt}^{-1} min^{-1}, the apparent activation energy (Ea) values, and the stability of Pt-based catalysts used in hydrolysis of AB in literature. * AB was added into the reaction solution without separating the catalyst. Note that the size and surface area of the catalysts were provided for comparison.

No.	Catalyst	Pt wt %	mol_{metal}/mol_{AB}	Surface area(m^2/g)	T (°C)	Ea (kJ/mol)	TOF (mol_{H2} mol_{Pt}^{-1} min^{-1})	Stability	Ref
1	Pt_1/Co_3O_4-c	0.05	0.0016	14.9	30	35.7	6035	10. Run (%97)	This work
2	$Pt^0/CoFe_2O_4$	0.23	0.000058	55	30	65	4900	10.Run (%100)	13
3	Pt^0/Co_3O_4	0.24	0.0000615	43	25	71	4366	10.Run (%100)	14
4	Pt_2/graphene	0.72	0.00011	-	27	-	2800	5.Run (%100)	15
5	Pt_1/Co_3O_4	0.5	-	-	25	37.4	1220	10.Run (%93)	9
6	R-PtNi/NiO@SiO_2	0.48	-	220	30	43	1217	5.Run (%100)	16
7	Pt/Co_3O_4	9.8	-	137	25	31.3	721	10.Run (%86.7)	17
8	Pt/CNT-5W	1.3	-	-	30	27.8	710	5.Run (%100)	18
9	$PtCo_{20}$/CNTs	0.98	-	-	25	42.5	675	-	19
10	Pt_4Ni_1-NPs	-	-	-	-	-	638	-	20
11	$PtNiO_xTV_o$	-	-	-	25	59.3	618	10.Run（%85）	21
12	Pt/CNTs-O-HT	1.5	0.0047	221	30	-	567	-	22
13	$K_2[PtCl_6]$	-	-	-	25	29	558	5.Run (%68)	23
14	PEI–GO/$Pt_{0.17}Co_{0.83}$	-	0.0027	-	25	51.6	378	5.Run (%80)	24
15	Pt-NPs/Co_3O_4	13.5	-	-	25	-	349	10.Run (%38)	9
16	$Pt_{25}@TiO_2$	13.5	0.0016	45	25	-	311	3.Run (%75)	25
17	Pt-MUAte	-	-	-	20	-	~220	-	26
18	Pt1/graphene	0.35	0.00011	-	27	-	160	-	15
19	NP-$Pt_{40}Co_{60}/Co_3O_4$	-	-	-	25	38.8	135	5.Run (%70)	27
20	Pt/activated carbon	3.0	0.0047	-	25	-	127	-	22

Table S3. The structure parameters of the optimized Co_3O_4-(100), Co_3O_4-(111), Pt_1/Co_3O_4-(100), and Pt_1/Co_3O_4-(111) model and the AB adsorption models, H_2 adsorption models on the Co_3O_4-(100), Co_3O_4-(111), Pt_1/Co_3O_4-(100) and Pt_1/Co_3O_4-(111) surfaces. (The active Co sites in this corresponded to the Pt site.)

Surface	Path	Surface model	AB adsorption model	H_2 adsorption model
		R (Å)	R (Å)	R (Å)
Co_3O_4-(100)	Co–O1	1.86	1.91	1.90
	Co–O2	1.87	1.92	1.89
	Co–O3	1.93	1.91	1.90
	Co–O4	1.91	1.90	1.91
	Co–O5	2.07	1.93	1.92
	Co–H1 a	- -	1.65	- -
	B–H1 a	- -	1.28	- -
	Co–H1 b	- -	- -	1.81
	Co–H2 b	- -	- -	1.81
	H1–H2 b	- -	- -	0.78
Co_3O_4-(111)	Co–O1	1.77	1.83	1.89
	Co–O2	1.77	1.92	1.77
	Co–O3	1.77	1.81	1.78
	Co–H1 a	- -	1.65	- -
	B–H1 a	- -	1.37	- -
	Co–H1 b	- -	- -	1.99
	Co–H2 b	- -	- -	1.98
	H1–H2 b	- -	- -	0.77
Pt_1/Co_3O_4-(100)	Pt–O1	1.98	2.04	2.03
	Pt–O2	1.98	2.02	2.04
	Pt–O3	2.03	2.03	2.04
	Pt–O4	2.03	2.03	2.03
	Pt–O5	2.03	2.08	2.00
	Pt–H1 a	- -	1.65	- -
	B–H1 a	- -	1.37	- -
	Pt–H1 b	- -	- -	1.71
	Pt–H2 b	- -	- -	1.71
	H1–H2 b	- -	- -	0.87
Pt_1/Co_3O_4-(111)	Pt–O1	1.90	1.95	1.90
	Pt–O2	1.90	2.07	1.89
	Pt–O3	1.90	1.98	1.89
	Pt–H1 a	- -	1.65	- -
	B–H1 a	- -	1.37	- -
	Pt–H1 b	- -	- -	3.31
	Pt–H2 b	- -	- -	3.27
	H1–H2 b	- -	- -	0.75

a: The bonds were in the AB adsorption model on the Co_3O_4-(100), Co_3O_4-(111), Pt_1/Co_3O_4-(100), and Pt_1/Co_3O_4-(111) surfaces. b: The bonds were in the AB adsorption model on the Co_3O_4-(100), Co_3O_4-(111), Pt_1/Co_3O_4-(100),

and Pt_1/Co_3O_4-(111) surfaces.

Table S4. The Bader charge of Pt atom of Pt_1/Co_3O_4-(100), and Pt_1/Co_3O_4-(111) surfaces. And the adsorption energy of the optimized AB adsorption models, H_2 adsorption models on the Co_3O_4-(100), Co_3O_4-(111), Pt_1/Co_3O_4-(100), and Pt_1/Co_3O_4-(111) surfaces.

Samples	Bader Charge of Pt	$E_{ads\text{-}AB}$ (eV)	$E_{ads\text{-}H2}$ (eV)
Co_3O_4-(100)		–0.56	–0.75
Co_3O_4-(111)		–1.33	–0.67
Pt_1/Co_3O_4-(100)	+1.24 |*e*|	–1.69	–0.65
Pt_1/Co_3O_4-(111)	+1.04 |*e*|	–0.67	0.00

$E_{ads\text{-}AB}$: the adsorption energy of AB; $E_{ads\text{-}H2}$: the adsorption energy of H_2.

Reference:

1 X. Xiao, X. Liu, H. Zhao, D. Chen, F. Liu, J. Xiang, Z. Hu and Y. Li, *Adv. Mater.*, 2012, **24**, 5762-5766.

2 M. Kang, H. Zhou, D. Wu and B. Lv, *CrystEngComm*, 2016, **18**, 9299-9306.

3 B. Qiao, A. Wang, X. Yang, L. F. Allard, Z. Jiang, Y. Cui, J. Liu, J. Li and T. Zhang, *Nat. Chem.*, 2011, **3**, 634-641.

4 G. Kresse and J. Hafner, *Phys. Rev. B. Condens. Matter*, 1993, **47**, 558-561.

5 G. Kresse and J. Hafner, *Phys. Rev. B. Condens. Matter*, 1994, **49**, 14251-14269.

6 G. Kresse and J. Furthmuller, *Phys. Rev. B. Condens. Matter*, 1996, **54**, 11169-11186.

7 G. Kresse and J. Furthmüller, *Comput. Mater. Sci.*, 1996, **6**, 15-50.

8 J. P. Perdew, K. Burke and M. Ernzerhof, *Phys. Rev. Lett.*, 1996, **77**, 3865-3868.

9 J. Li, Q. Guan, H. Wu, W. Liu, Y. Lin, Z. Sun, X. Ye, X. Zheng, H. Pan, J. Zhu, S. Chen, W. Zhang, S. Wei and J. Lu, *J. Am. Chem. Soc.*, 2019, **141**, 14515-14519.

10 S. Gao, Z. Sun, W. Liu, X. Jiao, X. Zu, Q. Hu, Y. Sun, T. Yao, W. Zhang, S. Wei and Y. Xie, *Nat. Commun.*, 2017, **8**, 14503.

11 J. Deng, W. Song, L. Chen, L. Wang, M. Jing, Y. Ren, Z. Zhao and J. Liu, *Chem. Eng. J.*, 2019, **355**, 540-550.

12 R. F. W. Bader, *Chem. Rev.*, 1991, **91**, 893-928.

13 S. Akbayrak and S. Ozkar, *J. Colloid Interface Sci.*, 2021, **596**, 100-107.

14 S. Akbayrak and S. Ozkar, *ACS Appl. Mater. Interfaces*, 2021, **13**, 34341–34348.

15 H. Yan, Y. Lin, H. Wu, W. Zhang, Z. Sun, H. Cheng, W. Liu, C. Wang, J. Li, X. Huang, T. Yao, J. Yang, S. Wei and J. Lu, *Nat. Commun.*, 2017, **8**.

16 Y. Ge, W. Ye, Z. H. Shah, X. Lin, R. Lu and S. Zhang, *ACS Appl. Mater. Interfaces*, 2017, **9**, 3749-3756.

17 M. Li, S. Zhang, J. Zhao and H. Wang, *ACS Appl. Mater. Interfaces*, 2021, **13**, 57362−57371.

18 W. Chen, W. Fu, G. Qian, B. Zhang, Chen, X. Duan and X. Zhou, *iScience*, 2020, **23**, 100922.

19 J. Zhang, W. Chen, H. Ge, C. Chen, W. Yan, Z. Gao, J. Gan, B. Zhang, X. Duan and Y. Qin, *Appl. Catal., B*, 2018, **235**, 256-263.

20 S. Wang, D. Zhang, Y. Ma, H. Zhang, J. Gao, Y. Nie and X. Sun, *ACS Appl. Mater. Interfaces*, 2014, **6**, 12429-12435.

21 R. Shen, Y. Liu, H. Wen, X. Wu, G. Han, X. Yue, S. Mehdi, T. Liu, H. Cao, E. Liang and B. Li, *Small*, 2022, **18**, e2105588.

22 W. Chen, J. Ji, X. Duan, G. Qian, P. Li, X. Zhou, D. Chen and W. Yuan, *Chem. Commun.*, 2014, **50**, 2142-2144.

23 N. Mohajeri, A. T-Raissi and O. Adebiyi, *J. Power Sources*, 2007, **167**, 482-485.

24 M. Li, J. Hu, Z. Chen and H. Lu, *RSC Adv.*, 2014, **4**, 41152-41158.

25 M. A. Khalily, H. Eren, S. Akbayrak, H. H. Susapto, N. Biyikli, S. Ozkar and M. O. Guler, *Angew. Chem., Int. Ed.*, 2016, **55**, 12257-12261.

26 M. Monai, T. Montini, E. Fonda, M. Crosera, J. Jose Delgado, G. Adami and P. Fornasiero, *Appl. Catal., B*, 2018, **236**, 88-98.

27 Q. X. Zhou and C. X. Xu, *J. Colloid Interface Sci.*, 2017, **508**, 542-550.